Chemical Engineering Journal 108 (2005) 59–67

Chemical Engineering Journal

www.elsevier.com/locate/cej

Experimental study of particle flow in a gas–solid separator with baffles using PDPA

L. Du, J. Zh. Yao, W.G. Lin *

Multi-phase Reaction Laboratory, Institute of Process Engineering, Chinese Academy of Sciences, P.O. Box 353, Beijing 100080, PR China

Received 9 August 2004; received in revised form 4 December 2004; accepted 22 December 2004

Abstract

Particle flow behavior in a gas–solid separator with a guide baffle and separation baffles developed by the Institute of Process Engineering (IPE) for cocurrent down-flow reactors has been studied with a Phase Doppler Particle Analyzer (PDPA), which allows to measure the particle size and velocity simultaneously. Profiles of particle velocities, particle size and particle number density at different heights in the separator were obtained. Analysis of the velocity profile indicates that the particle inertia has a significant effect on the behavior of particles in different size groups: the trajectories of the smaller particles are more influenced by the gas stream in relation to the larger, more heavier, particles. Experimental results reveal that the guide baffle together with the separation baffles plays a role of guidance as well as particle concentrators. Particles entrained by the gas flowing upward along the top side of the separation baffle may mainly come from the regions far from the guide baffle surface. Small particles are gradually dispersed toward the periphery of the two-phase flow field after being ejected from the rectangular nozzle, giving rise to a bimodal behavior of particle size distributions in the region far from the guide baffle.

Keywords: Down-flow reactor; Gas–solid separator; Particle flow; PDPA

1. Introduction

In the last decade, more and more attention have been paid to co-current down-flow circulating fluidized bed reactors, so called ‘downer’ reactors. These reactors found a wide application, including fluidized catalytic cracking processes [1–3], ultra-pyrolysis of cellulose biomass [4], gasification and liquefaction of coal [5,6]. The downer reactors offer significant advantages over the risers and conventional fluidized bed reactors for fast reactions due to its much more uniform gas–solid flow pattern, shorter contact time, low axial dispersion, higher solids/gas loading ratio, and ability to operate at a higher temperature [7]. For fast reactions with only a fraction of a second of gas–solid reaction/residence time, the quick separation of gas and solids at the outlet of the downer is, therefore, essential to prevent the overreaction occurrence and to ensure good productivity. A cyclone, with the residence time of the order of 1–2 s, may not be feasible for a downer reactor. Non-traditional gas–solids separators, with low residence time and high separation efficiency, are required.

A short residence time gas–solids separation device has been patented by Stone & Webster Engineering Corporation [8]. It is a U-turn inertial separator. Separation is effected by projecting solids by centrifugal force against a bed of solids as the gas phase makes a 180° directional change and solids only 90° change relative to the incoming stream. By formation of the one-quarter-curve bed of solids, erosion of the wall opposite the inlet of the separator is eliminated and a U-shaped 180° flow pattern of the gas stream is aided to establish. Although a very short residence time were claimed for the separator, the separation efficiency was not high enough due to significant gas entrainment.

For the same purpose, another gas–solid separator for downer reactors has been developed by Tsinghua University in the 1980s [9]. It is a simple inertial separator in which gas and solids suspension first pass through a specially designed

* Corresponding author. Tel.: +86 1062572591; fax: +86 1062561822.
E-mail address: wglin@home.ipe.ac.cn (W.G. Lin).

1385-8947/$ – see front matter © 2005 Elsevier B.V. All rights reserved.
doi:10.1016/j.cej.2004.12.043

nozzle and then impinge on a curved guiding plate with a gradually increasing radius.

Recently, the Institute of Process Engineering, Chinese Academy of Sciences, has proposed a novel gas–solid separator, the Combined Baffles Quick-Separation Device (CBQSD), which has been applied to flash pyrolysis of coal in a downer. Previous experimental results have shown that the CBQSD has some advantages, such as high separation efficiency, low-pressure loss, especially its relatively compact and symmetric structure [10]. It has also been found that separation performances (separation efficiency, pressure drop, etc.) largely depend on geometrical parameters. The optimum design and scale-up of the CBQSD requires a thorough understanding of gas–solid flow patterns. To achieve this understanding, detailed experimental measurements of the gas–solid flow provide a basic tool.

Many techniques have been used for characterizing multiphase flow patterns, including X-ray densitometer [11], γ-ray computed tomography [12,13], electrical capacitance tomography [14,15], Laser Doppler Anemometry [16] and Particle Image Velocimetry (PIV) [17], etc.

In the present paper, the solid-phase hydrodynamics in the CBQSD was studied by using a Phase Doppler Particle Analyzer (PDPA). The PDPA is a non-intrusive, laser-based measurement technique based on measuring the Doppler signal scattered by the particle as it cross the sample volume. It allows the simultaneous measurement of size and velocity of spherical particles, droplets, or bubbles. Until now, this measuring technique has been successfully used for particle measurements in a wide variety of situations, such as swirling flow [18,19] and gas-particle flow in a circulating fluidized bed [20].

The objective of this study is to understand the separation mechanism of the newly developed separator CBQSD and to investigate the solid-phase hydrodynamics under a given operating and geometrical conditions with a two-component PDPA to obtain particle size, velocity and number density.

2. Experimental details

Experiments were carried out in a setup consisting of a riser, a downer and a gas–solid separator, which is schematically shown in Fig. 1. An air compressor supplied air to a two-dimensional separator (CBQSD) via a riser with 32 mm inner diameter and a downer with 40 mm inner diameter. The riser and the downer had the same height of 3 m. The airflow rate was controlled by a valve and a flow meter. Glass beads were loaded into the airflow by a feeding system consisting of a valve and a particle container. After gas–solid separation, the separated particles entered into a solids tank below the separator, while the unseparated particles were entrained out of the separator by the gas flow and were collected by bag-type collectors.

The geometrical structure of the two dimensional separator is shown in Fig. 2a. The separator consists of three internal

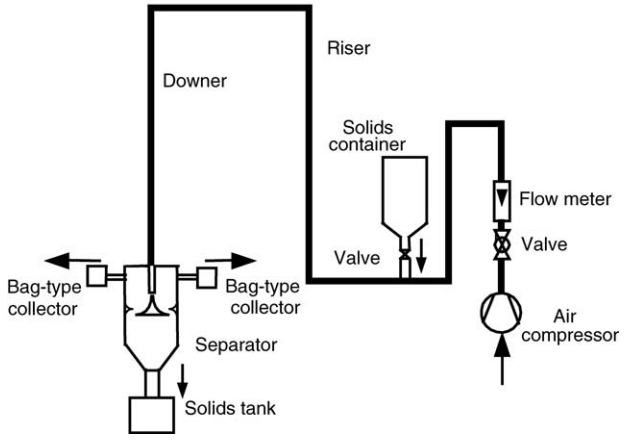

Fig. 1. Schematic of the experimental apparatus.

components: a rectangular nozzle (RN) which introduces the gas–solid flow into the separator, a guide baffle (GB) which is composed of two circular arcs in bilateral symmetry, and a separation baffle (SB) which is also composed of two circular arcs, SB-top and SB-bottom, but in up-down symmetry. Compared with the downer tube, the rectangular nozzle has a smaller cross-section. The separator is made of Plexiglas, which enables PDPA measurements possible.

The particle size, velocity and number density in the separator were measured by an Aerometrics two-component PDPA. The principle of PDPA was described by Bachalo and Houser [21]. The arrangement of the measuring system is shown in Fig. 2b.

In the measuring system, particle size is determined by using green beams with a wavelength of 0.5145 μm, which also give the first component of particle velocity, i.e., the vertical velocity u, while the 0.488 μm blue beams provide the second orthogonal component of particle velocity, i.e., the transversal velocity v. The selected optical components are a transmitter lens, a receiver lens with $f = 500$ mm and receiver back lens with $f = 238.6$ mm. The combination gives an effective detecting range of 0.5–142 μm of the particle size. For glass beads the PDPA was configured in the 22° off-axis forward scatter for this study.

Experimental conditions are listed in Table 1 and the particle-size distribution measured at one point of the nozzle outlet by a PDPA is also given in Fig. 3.

Particle behavior near the guide baffle and the separation baffles were of our major interest. Thus, measurements in

Table 1
Flow conditions

Air flow	
Mean gas velocity (at the nozzle outlet) (m/s)	3.7
Reynolds number (obtained with nozzle $D_h = 24$ mm)	6000
Particles	
Particle arithmetic mean diameter (μm)	67
Particle material density (kg/m^3)	2500
Particle mass flow rate (g/s)	5.33
Particle loading	1.31

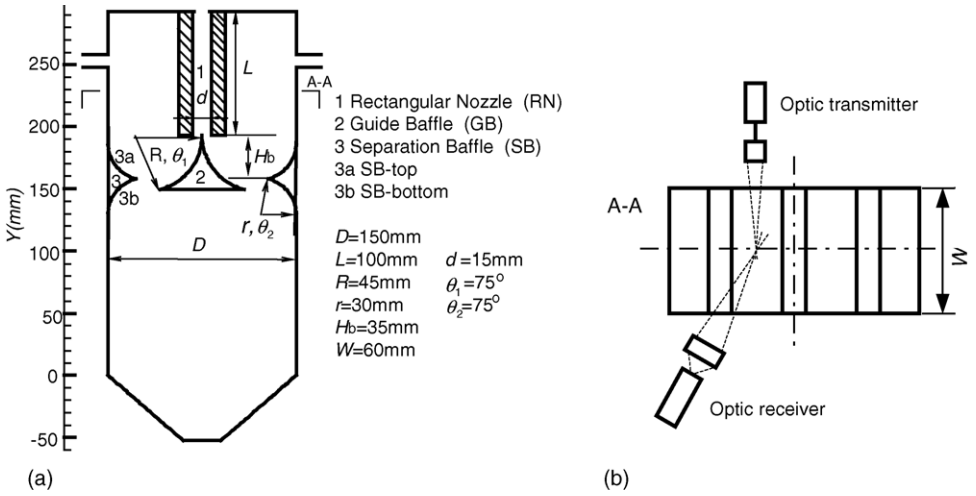

Fig. 2. Geometrical configuration of the separator. (a) Frontal bi-dimensional scheme of the separator geometry and (b) scheme of the PDPA measuring system.

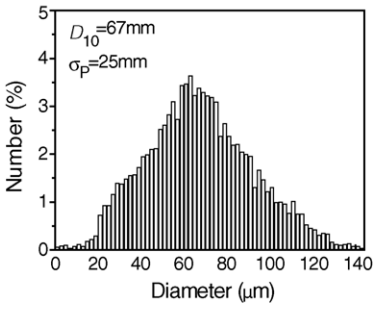

Fig. 3. Particle size distribution.

this study were focused on those regions. Experiments were performed with transversal scans at nine different heights, $Y = 190, 180, 175, 170, 165, 160, 155, 150, 140$ mm (Fig. 2a), to obtain particle velocity, particle size and particle number density in the separator. At each height, the distance between measurement points was kept 1 or 2 mm. The measurements started at the point as close to the surface of the GB and SB as possible. When the particle number density was very low at the point far from the surface, the PDPA measurements were stopped. In order to achieve reasonably accurate local mean parameters (velocity, size, etc.) of the particle behaviors, twenty thousand particles were measured at each location.

3. Experimental results and discussion

3.1. Particle velocity

3.1.1. Particle mean velocity vectors in the separator

Fig. 4 plots particle mean velocity vectors that indicate the motion of particles in the separator. The two components of the particle mean velocity vectors, the vertical and horizontal, represent particle mean vertical and transversal velocity, respectively, averaged over all particle sizes. The positive directions of particle vertical and transversal velocity are defined to be vertically upward and horizontally right, respectively. In Fig. 4, it is observed that particles flow vertically downward from the inlet rectangular nozzle along to the guide baffle. At the end of this baffle, some particles move downward due to the inertia effect, being eventually settled down. Other particles flow upward along the SB-top being entrained out of the separator by the gas flow. Conclusions could be drawn that in the gas–solid separation process the guide baffle and the separation baffles act as the guides, which change and direct the motion of the particles in the separator.

For the convenience of further study, different horizontal co-ordinate OX_1, OX_2, OX_3 are adopted for the guide baffle, and top and bottom regions of the separation baffles, respectively, as shown in Fig. 4. The origins are set at the intersection of horizontal co-ordinate and baffle surfaces. So, the co-ordinate at one point near the guide baffle surface, X_1 of

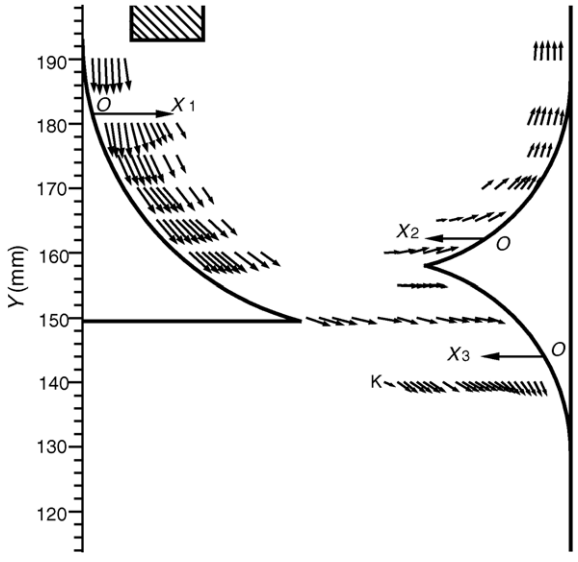

Fig. 4. Particle mean velocity vectors in the separator.

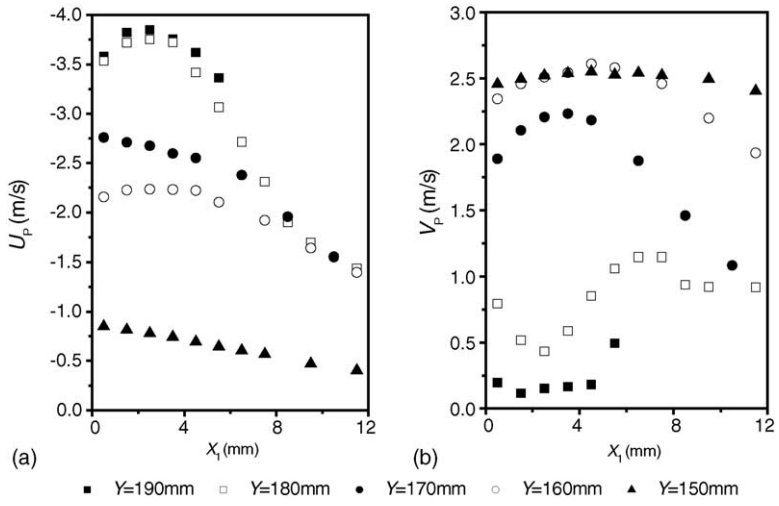

Fig. 5. Profiles of particle mean vertical velocity (a) and mean transversal velocity (b) along the guide baffle from $Y = 190$ to 150 mm.

the OX_1-axis, for instance, represents the horizontal distance from the point to the guide baffle surface.

3.1.2. Particle velocity near the guide baffle

Fig. 5 shows the profiles of particle mean vertical U_P (a) and transversal V_P (b) velocities averaged over all particle sizes along the guide baffle for heights from $Y = 190$ to 150 mm, respectively. At all heights the vertical velocity is high close to the guide baffle; whereas lower in the region far from the guide baffle. Also, noticeable is that the particles exhibit a decrease in vertical velocity along the guide baffle from $Y = 190$ to 150 mm but variations of the particle vertical velocity between two neighboring vertical locations are different: largest between $Y = 160$ and 150 mm, while smallest between $Y = 190$ and 180 mm. However, for the transversal velocity profiles (Fig. 5a) this is not the case at all. The profiles are quite different between each other. In the transversal direction, the particles are accelerated along the guide baffle. There is a lowest value of transversal velocity in the region close to the guide baffle at $Y = 190$ and 180 mm, quite different from the profiles at $Y = 170$ and 160 mm where a highest value is found in the region close to the guide baffle. The reason for this behavior is that after being ejected downward from the nozzle with almost zero transversal velocity, the particles which are located in the region closest to the guide baffle will first collide with the guide baffle and then rebound, attaining a high transversal velocity value. The particles located far from the guide baffle increase gradually their transversal velocity due to the drag force exerted by the gas flow. As a result, a lowest value of transversal velocity is obtained in the region close to the guide baffle at $Y = 190$ and 180 mm. At the end of the guide baffle, i.e., $Y = 150$ mm, an almost uniform distribution of transversal velocity is seen.

To investigate the behavior of different size particles, the data of particle size and velocity are reprocessed after the measurements. The particle size distribution in the range from 30 to 100 μm is resolved by seven classes of 10 μm width. In Fig. 6, the mean vertical velocity is shown for four particle size classes (35, 55, 75 and 95 μm) of 10 μm width at five heights near the guide baffle. It is seen that at $Y = 190$ mm which is very close to the outlet of the rectangular nozzle the smaller the particles are, the higher the vertical velocity is,

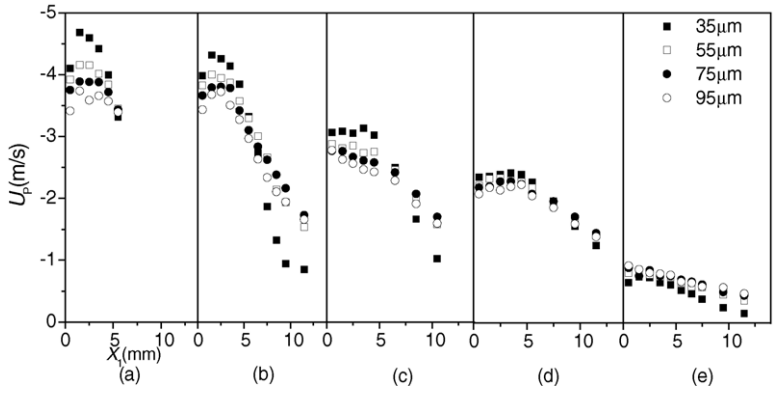

Fig. 6. Distributions of mean vertical velocity of different size particles at (a) $Y = 190$ mm, (b) $Y = 180$ mm, (c) $Y = 170$ mm, (d) $Y = 160$ mm and (e) $Y = 150$ mm near the guide baffle.

probably caused by faster acceleration for the smaller particles due to their lower inertia in the 100 mm rectangular nozzle.

From this location until $Y = 160$ mm, the smaller particles still have larger vertical velocity in the region close to the guide baffle. However, the differences of vertical velocity among different size particles are gradually decreasing. The small particles are decelerated so fast that when they reach the end of the guide baffle, i.e., $Y = 150$ mm, their vertical velocities are below large particles' vertical velocities, as shown in Fig. 6e. It is also observed that in the region far from the guide baffle at $Y = 180$ and 170 mm the smaller particles (35 μm) have lower velocity. A possible reason for above behavior of smaller particles is given as the following.

One possible explanation is due to the change in the gas velocity. Observing the geometry of the guide baffle it is reasonable to assume that the vertical component of the gas vector velocity will decrease with the co-ordinate Y diminution. Considering that the smaller particles have a lower inertia, it can be assumed that these particles will be more influenced by the gas flow, than the larger ones. This behavior will lead to a more notably mean diminution of the smaller particles vertical velocity in comparison with the larger particles.

3.1.3. Particle velocity near the SB-top and SB-bottom

Fig. 7 shows the profiles of vertical mean velocity (a) and transversal mean velocity (b) averaged over all particle sizes along the SB-top from $Y = 160$ to 190 mm. It can be seen from Fig. 7 that when going upward along the SB-top surface, the particles reveal an increase in vertical velocity but a decrease in transversal velocity.

Fig. 8 shows the distributions of mean vertical velocity at (a) $Y = 160$ mm, (b) $Y = 170$ mm, (c) $Y = 180$ mm, (d) $Y = 190$ mm near the SB-top for five particle size classes, namely, 15, 35, 55, 75, 95 μm. As shown in Fig. 7a, all the particles are accelerated along the SB-top. In Fig. 8, it is observed that at each height smaller particles generally exhibit higher vertical velocity. This behavior is probably caused by its lower inertia, being more accelerated due to the drag force effect of the gas flow. The profiles of mean vertical velocity of

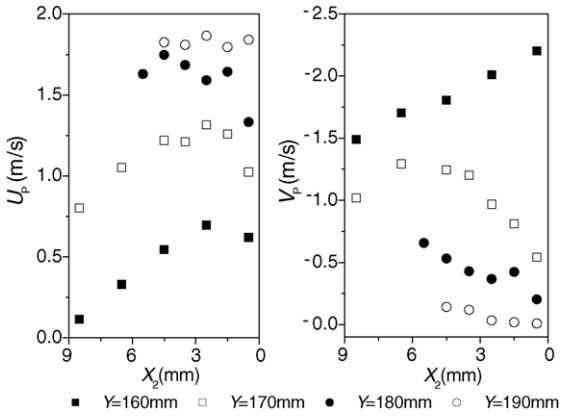

Fig. 7. Profiles of particle mean vertical velocity (a) and mean transversal velocity (b) along the SB-top from $Y = 160$ to 190 mm.

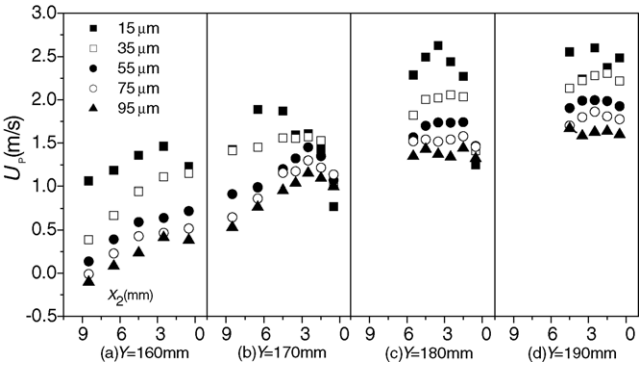

Fig. 8. Distributions of mean vertical velocity of different size particles near the SB-top at (a) $Y = 160$ mm, (b) $Y = 170$ mm, (c) $Y = 180$ mm, (d) $Y = 190$ mm.

different size particles near the separation baffle-top together with those near the guide baffle shown in Fig. 6 manifest the significant effects of inertia on the behavior of different size particles: smaller particles more rapidly respond to the change of the gas flow.

Fig. 9a illustrates the distribution of particle vertical velocity at $Y = 155$ mm near the SB-bottom for four size classes (35, 55, 75 and 95 μm). It should be noticed that small parti-

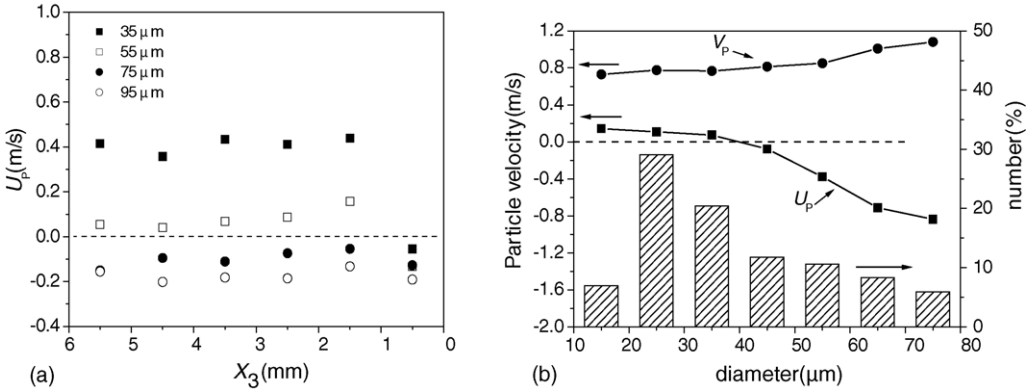

Fig. 9. (a) Particle mean velocity distributions near the SB-bottom at $Y = 155$ mm for 35, 55, 75, 95 μm particles (b) Particle mean velocity together with particle size distributions at a point K ($X_3 = 24.5$ mm, $Y = 140$ mm) shown in Fig. 4.

cles (i.e., 35, 55 μm) show a positive value of vertical velocity at $Y = 155$ mm near the SB-bottom, which means that the gas is flowing upward in this region, entraining small particles upward. However, larger particles show a negative vertical velocity at $Y = 155$ mm near the SB-bottom, where the velocity of gas flow may be too low to entrain the larger particles.

The behavior of the gas–solid flow at a point K near the SB-bottom ($X_3 = 24.5$ mm, $Y = 140$ mm) shown in Fig. 4 is shown in Fig. 9b. In this figure, is shown the particle mean velocity for different size classes from 10 to 80 μm associated with the particle size distribution. It is observed that at the point K the concentration of smaller particles is greater and larger particles have higher vertical and transversal (in module) velocities. The very low number density of the smaller particles with the mean diameter equal to 15 μm is in relation to the location of analyzed point K. If the analyzed point K is located much farther away from the surface of SB-bottom, the number density of 15 μm particles may be much higher. The smaller particles (i.e., 15, 25, 35 μm) exhibit a positive value of mean vertical velocity, which suggests that there can exist a gas recirculation in the region far from the SB-bottom.

3.2. Particle size

Fig. 10 shows the distributions of the arithmetic mean diameter D_{10} near the guide baffle at heights $Y = 190$ mm (a), $Y = 180$ mm (b), $Y = 170$ mm (c), $Y = 160$ mm (d), $Y = 150$ mm (e), near the SB-top at the height $Y = 160$ mm (f), and near the SB-bottom at the height $Y = 140$ mm (g). It can be observed that the arithmetic mean diameter D_{10} close to the guide baffle is generally larger than that far from the guide baffle at $Y = 190$ mm (a), $Y = 180$ mm (b), $Y = 170$ mm (c), $Y = 160$ mm (d) and $Y = 150$ mm (e), respectively. This implies that a larger number percent of small particles may be found in the region far from the guide baffle. Also, noticeable is that there is a significant increase in the arithmetic mean diameter near the guide baffle from $Y = 160$ mm (d) to $Y = 150$ mm (e), however, there is a significant decrease from $Y = 160$ mm (d) near the guide baffle to $Y = 160$ mm (f) near the SB-top. This suggests that when particles go along the guide baffle from $Y = 160$ mm to $Y = 150$ mm, some small particles are entrained by the gas flow to the SB-top. At the height $Y = 140$ mm (g), near the SB-bottom, the arithmetic mean diameter close to the SB-bottom is much larger than that far from the SB-bottom where small particles, accounting for larger fractions, may be found.

In an attempt to further explain the foregoing results, the evolutions of particle size distributions are depicted in Fig. 11 at three transversal points (three columns) for each of five heights (five rows), namely, near the guide baffle: $Y = 190$ mm (the first row), $Y = 180$ mm (the second row), $Y = 160$ mm (the third row), near the SB-top $Y = 160$ mm (the fourth row), near the SB-bottom $Y = 140$ mm (the fifth row). The first row shows that particles near the guide baffle at $Y = 190$ mm (which is very close to the outlet of the rectangular nozzle) are mono-modal distributions with peaks at about 70 μm. It should be noticed that at $Y = 180$ mm and $Y = 160$ mm near the guide baffle the particle size distributions vary gradually from a mono-modal distribution with a peak at 70 μm (left) to a bi-modal one with two peaks approximately at 30 μm (left) and 70 μm (right), which means the fraction of small particles increases with the increase of the distance to the guide baffle. The variations of particle size distributions clearly indicate that small particles are gradually dispersed toward the periphery of the two-phase flow field after being ejected from the rectangular nozzle. At all three points for $Y = 160$ mm, near the SB-top (the fourth row), particles show bimodal distributions with two peaks approximately at 30 and 70 μm, probably relating to the bimodal behaviors mentioned above at locations far from the guide baffle for the heights $Y = 160$ and 180 mm. This means that some particles entrained by the gas flow at $Y = 160$ mm near the SB-top may come from the regions far from the guide baffle. For the height $Y = 140$ mm (the fifth row) near the SB-bottom particles show the same evolution behavior as at $Y = 180$ and 160 mm near the guide baffle: small particles are becoming more and more as X_3 increases. Especially at $X_3 = 24.5$ mm particles mainly consists of small ones which move upward as already indicated in Fig. 9b.

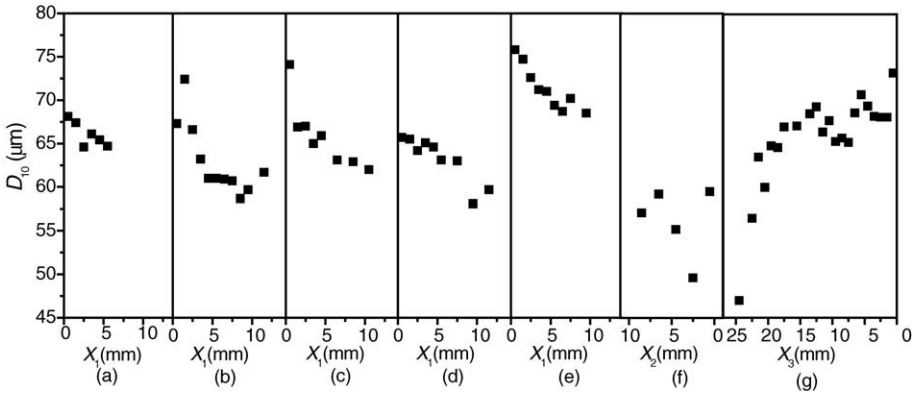

Fig. 10. Distributions of the arithmetic mean diameter near the guide baffle at heights $Y = 190$ mm (a), $Y = 180$ mm (b), $Y = 170$ mm (c), $Y = 160$ mm (d), $Y = 150$ mm (e), near the SB-top at the height $Y = 160$ mm (f) and near the SB-bottom at the height $Y = 140$ mm (g).

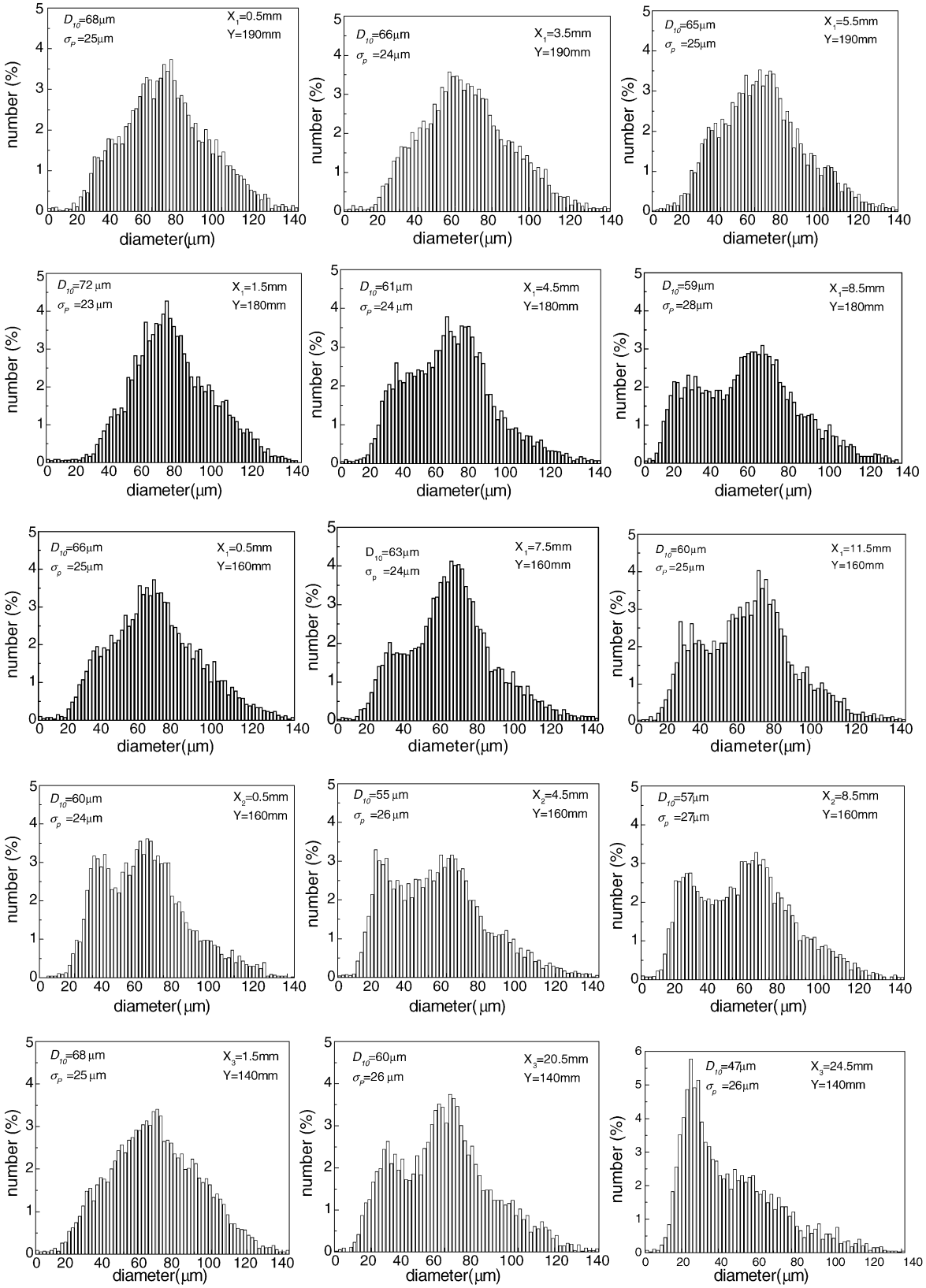

Fig. 11. Evolutions of particle size distributions at three transversal positions (three columns) for each of five heights (five rows), namely, near the guide baffle: $Y = 190$ mm (the first row), $Y = 180$ mm (the second row), $Y = 160$ mm (the third row), near the SB-top $Y = 160$ mm (the fourth row) and near the SB-bottom $Y = 140$ mm (the last row).

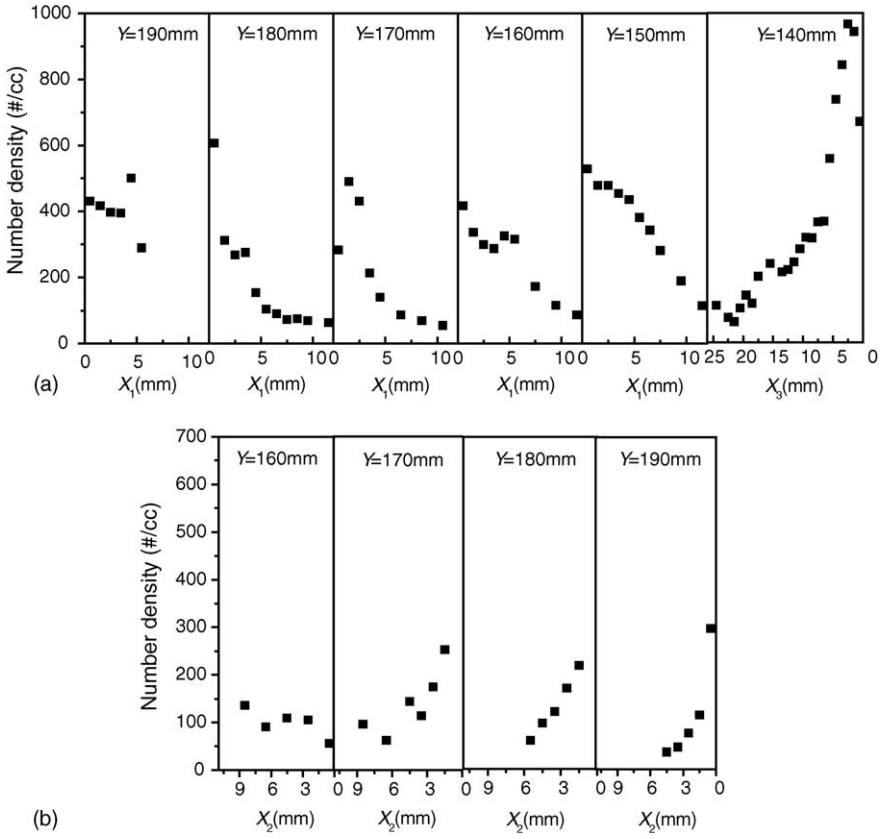

Fig. 12. Particle number density distributions (a) near the guide baffle at $Y = 190$, 180, 170, 160, 150 mm and near the SB-bottom at $Y = 140$ mm, (b) near the SB-top at $Y = 160$, 170, 180, 190 mm.

3.3. Particle number density

Fig. 12 illustrates the transversal distributions of particle number density at different heights in the separator CBQSD. It can be observed from Fig. 12a that near the guide baffle at $Y = 190$ mm particles are narrowly contained within the outlet of the rectangular nozzle. When particles reach the height of $Y = 180$ mm near the guide baffle, a wider number density distribution is found. Close to the guide baffle the particle concentration is high; however, the number density decays quickly as the distances to the guide baffle X_1 increases. So, are the distributions for heights at $Y = 170$, 160 and 150 mm near the guide baffle. The number density distributions near the guide baffle imply that after being ejected from the rectangular nozzle, although a few number of particles are dispersed into the regions far from the guide baffle, most of them are still concentrated close to the guide baffle due to inertia effects. It can also be seen from Fig. 12a that at $Y = 140$ mm near the SB-bottom with the distance to the SB-bottom X_3 increasing, the number density reduces sharply, which means that after particles leave the guide baffle at $Y = 150$ mm where particles are mainly concentrated close to the guide baffle, they gather very close to the SB-bottom again.

Fig. 12b shows the particle number density distributions near the SB-top at different heights. At $Y = 160$ mm, a slightly high particle number density is found far from the SB-top, while particle concentrations are relatively high close to the SB-top for each height of $Y = 170$, 180 and 190 mm. The reason is probably that particles, which move farther from the guide baffle at $Y = 160$ mm are more easily and largely entrained by the U-turn gas flow than those closer to the guide baffle. When going along the SB-top from $Y = 170$ to 190 mm, a large number of particles entrained by the upward gas flow concentrate again close to the SB-top due to the inertial effect.

From the above discussions, it can also be concluded that besides guidance, the guide baffle and the baffles, including the SB-top and the SB-bottom also play a role of particle concentrator, which make the particles gather close to their surfaces and are favorable to the gas–solid separation process.

4. Conclusions

The particle flow behavior in a gas–solid separator with a guide baffle and separation baffles developed by the Institute of Process Engineering (IPE) for co-current down-flow reactors have been studied with a Phase Doppler Particle Analyzer. Profiles of particle velocities, particle size and particle number density at different heights in the separator were obtained and analyzed.

When the mean vertical and transversal velocity profiles are concerned, the results obtained show that along the guide baffle the particles are decelerated in vertical mean velocity but accelerated in mean transversal velocity; on the other hand, along the SB-top the particles are accelerated in vertical velocity but decelerated in transversal velocity. The inertia of particles has a significant effect on the behavior of particles in different size groups, which means that smaller particles are more influenced by the drag force of the gas stream.

Results reveal that the guide baffle together with the separation baffles play a role of guidance as well as particle concentrators, which are very important to the gas–solid separation process. Particles entrained by the gas flow upward along the SB-top may mainly come from the regions far from the guide baffle. Small particles are gradually dispersed toward the periphery of the two-phase flow field after being ejected from the rectangular nozzle, giving rise to a bimodal behavior of particle size distributions in the region far from the guide baffle.

In the present paper, PDPA measurements were performed under a given operating and geometrical conditions. The influence of the baffles' geometrical form, the gas mass flow rate and turbulence on the particle hydrodynamics was not taken into consideration. In order to fully understand the separation mechanism, further study of the influence of these factors on the particle hydrodynamics using PDPA need to be carried out.

Acknowledgements

The authors acknowledge with gratitude the financial support of the National Program of High Technology Research and Development (No. 2003AA514023 and No. 2001AA529010) and the National Natural Science Foundation of China (No. 20221603 and No. 90210034).

References

[1] J.A. Talman, L. Reh, An experimental study of fluid catalytic cracking in a downer reactor, Chem. Eng. J. 84 (3) (2001) 517.
[2] A.G. Maadhah, M. Abul-Hamayel, A.M. Aitani, T. Ino, T. Okuhara, Down-flowing FCC reactor, Oil Gas J. 98 (33) (2000) 66.
[3] J.A. Talman, R. Geier, L. Reh, Development of a downer reactor for fluid catalytic cracking, Chem. Eng. Sci. 54 (13–14) (1999) 2123.
[4] B.A. Freel, R.G. Graham, M.A. Bergougnou, R.P. Overend, L.K. Mok, Kinetics of the fast pyrolysis (ultrapyrolysis) of cellulose in a fast fluidized bed reactor, AIChE Symp. Ser. 83 (1987) 105.
[5] Y.J. Kim, S.H. Lee, S.D. Kim, Coal gasification characteristics in a downer reactor, Fuel 80 (13) (1915).
[6] C.D. Oberg, A.Y. Falk, Coal liquefaction by flash hydropyrolysis, Coal Process Technol. 6 (1980) 159.
[7] J.X. Zhu, Z.Q. Yu, Y. Jin, J.R. Grace, A. Issangya, Cocurrent downflow circulating fluidized bed (downer) reactors-a state of the art review, Can. J. Chem. Eng. 73 (1995) 662.
[8] R. J. Gartside, H. N. Woebcke, Low residence time gas–solid separation device and system, USA Patent: 4556541, 1985-12-03.
[9] C.M. Qi, Z.Q. Yu, Y. Jin, X.L. Cui, X.X. Zhong, A novel inertial separator for gas–solid suspension in concurrent downflow, Pet. Refining 12 (1989) 51 (in Chinese).
[10] S.G. Li, W.G. Lin, J. Zh. Yao, Novel separator for gas–solids cocurrent down-flow reactors, Chin. J. Process Eng. 2 (1) (2002) 12.
[11] A. Miller, D. Gidaspow, Dense, vertical gas–solid flow in a pipe, AIChE J. 38 (11) (1992) 1801.
[12] S. Roy, J.W. Chen, S.B. Kumar, M.H. Al-Dahhan, M.P. Dudukovic, Tomographic and particle tracking studies in a liquid–solid riser, Ind. Eng. Chem. Res. 3611 (1997) 4666.
[13] T. Schiewe, K.E. Wirtha, O. Molerusa, K. Tuzlaa, A.K. Sharmab, J.C. Chenb, Measurements of solid concentration in a downward vertical gas–solid flow, AIChE J. 45 (5) (1999) 949.
[14] A.J. Jaworski, T. Dyakowski, Application of electrical capacitance tomography for measurement of gas–solids flow characteristics in a pneumatic conveying system, Meas. Sci. Technol. 12 (8) (2001) 1109.
[15] Zh.Y. Huang, B.L. Wang, H.Q. Li, Dynamic voidage measurements in a gas soild fluidized bed by electrical capacitance tomography, Chem. Eng. Commun. 190 (10) (2003) 1395.
[16] Y.F. Zhang, A. Hamid, Dilute fluidized cracking catalyst particles-gas flow behavior in the riser of a circulating fluidized bed, Powder Technol. 84 (3) (1995) 221.
[17] K. Miyazaki, G. Chen, F. Yamamoto, J. Ohta, Y. Murai, K. Horii, PIV measurement of particle motion in spiral gas–solid two-phase flow, Exp. Thermal Fluid Sci. 19 (4) (1999) 194.
[18] M. Sommerfeld, H.H. Qiu, Detailed measurements in a swirling particulate two-phase flow by a phase-Doppler anemometer, Int. J. Heat Fluid Flow 12 (1) (1991) 20.
[19] A. Brena de la Rosa, S.V. Sankar, G. Wang, W.D. Bachalo, Particle diagnostics and turbulence measurements in a confined isothermal liquid spray, J. Eng. Gas Turbines Power, Trans. ASME 115 (3) (1993) 499.
[20] T. Van den Moortel, E. Azario, R. Santini, L. Tadrist, Experimental analysis of the gas-particle flow in a circulating fluidized bed using a phase Doppler particle analyzer, Chem. Eng. Sci. 53 (10) (1998) 1883.
[21] W.D. Bachalo, M.J. Houser, Phase/Doppler spray analyzer for simultaneous measurements of drop size and velocity distributions, Opt. Eng. 23 (5) (1984) 583.